2B

PREDICTIVE RESPONSE COMPUTATIONS FOR VIBRATION TESTS AND EARTHQUAKE OF MAY 20, 1986 USING AN AXISYMMETRIC FINITE ELEMENT FORMULATION BASED ON THE COMPLEX RESPONSE METHOD AND COMPARISON WITH MEASUREMENTS - A SWISS CONTRIBUTION

E. Berger*, H. Fierz* and D. Kluge**

INTRODUCTION

Background

A research project on the validation of current soil-structure interaction (SSI) methodologies - jointly sponsored by the U.S. Nuclear Regulatory Commission (USNRC) and the Electric Power Research Institute (EPRI) - has been under way since the beginning of 1986. Argonne National Laboratory (ANL) is coordinating the project on behalf of the USNRC and issued a Statement of work (Ref. 1) to participating universities and national laboratories in April 1986.

Basler & Hofmann (B&H) as consultant in civil safety matters to the Swiss Federal Office of Energy, Nuclear Safety Department (HSK) became aware of this EPRI/USNRC Validation Project during the "Workshop on Soil-Structure Interaction" in Bethesda, Maryland (Ref. 2). Because the firm has made extensive use in the past 15 years of its in-house SSI computer codes in connection with seismic reviews of several nuclear installations in Switzerland, there was a great interest in this project to validate the firm's own SSI methodology. Therefore, the USNRC was asked whether a Swiss participation in the project would be possible.

The USNRC welcomed such a participation, so that EPRI/USNRC Validation Project could benefit from the experience of other countries with other methodologies. Subsequently, B&H prepared a proposal to HSK (Ref. 3) to fund an HSK Validation Project and to participate on the regulatory side in the overall project. This led to a coopera-

* Technical Staff, Basler & Hofmann, 8029 Zürich, Switzerland
** Project Manager, Federal Office of Energy, Nuclear Safety Department, 5303 Würenlingen, Switzerland

axisymmetric finite element computer program BHLUSH/BHBOUND (Ref. 5). The predicted response was reported in Progress Report for Phase 1 (Ref. 6) to ANL (overall project coordinator), HSK and USNRC. Work on Phase 1 continued from December 1986 to June 1987.

Phase 2. The measured vibration test data were received from ANL and the predicted response from Phase 1 was compared with the measurements. The differences were interpreted with the aid of parametric studies using the computer model established in Phase 1. Based on the results of these studies a refined model set C was developed. Phase 2 took place during July 1987.

Phase 3. The model set C from Phase 2 was then used to predict the response of the soil-structure system (containment model and surrounding soil) subjected to the earthquake motions recorded at a point in the free-field during the event of May 20, 1986. The same computer program as in Phase 1 was used. The results from Phases 2 and 3, i.e. the comparison of measured and predicted forced vibration responses, the results of the parametric studies, the development of model set C and the prediction of the earthquake response were reported in Progress Report for Phases 2 & 3 (Ref. 7) to ANL, HSK and USNRC. Phase 3 took place during August 1987, and the predicted earthquake response was sent to ANL on magnetic tape on August 31, 1987.

Phase 4. The measured earthquake response data were received from ANL at the beginning of October 1987 and compared with the predicted response from Phase 3. One additional parameter variation was investigated to interprete some of the differences observed. The results of the comparison and the parameter variation together with the major findings from Phases 1 through 3 were summarized in a Final Report for the HSK Validation Project (Ref. 8) to ANL, HSK and USNRC. This work together with the preparation of this paper was completed by the end of November 1987.

Content of Paper

In this paper are presented the major findings and results form the four phases of this project. The analysis methods and the model sets used in the predictive response computations are described in the next two sections. They are followed by a section each on the comparison of predictions with measurements for the forced vibration tests and for the earthquake of May 20, 1986. Finally, a section on conclusions completes this paper.

The variation of the ground motions both horizontally and vertically in the discretized region of the site is basically considered by means of the discretized finite element representation of the soil-structure system.

As far as the earthquake generated wave pattern in the ground is concerned, the motions in the discretized soil-structure system depend on the definition of the earthquake ground motion in the free-field, that is at the boundary of the discretized soil-structure system. The SSI-methodolgy used in this project can account for vertically propagating plane waves (shear- and compression waves) in the free-field only. A horizontal variation of the ground motion in the free-field is not possible. Hence, each point on the surface in the free-field has the same motion, which may be an acceptable approximation in the immediate region around a structure.

The three dimensional representation of the 1/4-scale containment model is given by the axysimmetric formulation of the structural model. Energy transmitting boundaries at the vertical edges of the discretized soil-cylinder assure the proper dissipation of energy created by the soil-structure interaction effects, i.e. radiation damping in a horizontal direction is considered. The bottom boundary of the finite element mesh consists of a rigid base. Hence, to account for proper radiation damping in the vertical direction, this boundary has to be chosen deep enough, so that the influence of reflecting waves on the response of the structure can be neglected.

In the following, a brief description of the free-field and the SSI-analysis methods used in this project are given.

Free-Field Analysis

The free-field analysis used in this project assumes vertically propagating plane waves in a horizontally layered soil deposit limited in depth by a rigid base (Ref. 12, 13). Laterally the layers extend to infinity. The computations were made with the computer code FLUSH.F77 (Ref. 9, 14). The objectives of the free-field analysis were threefold:

- Determine the strain-compatible dynamic soil properties in the free-field, so that the effects of the non-linear soil behaviour (primary non-linearity) can be accounted for in the SSI-analysis.
- Show the variation of the earthquake ground motion with depth in the free-field.
- Deconvolve the given earthquake acceleration time-histories in the free-field from the surface to the depth of the rigid base of the finite element mesh used in the SSI-analysis.

DESCRIPTION OF MODELS

General

An overview of the SSI model sets used in this project is given in Table 1, which contains for each model set the number of subsets used and their identification, the data packages available and explanatory comments.

Table 1

OVERVIEW OF SSI MODEL SETS USED IN HSK VALIDATION PROJECT

Model Set	No. of Subsets in Each Set	Subset Identification	Data Packages Used*	Comments
A	-	-	-	Not Considered in HSK Validation Project
B	4	B_1	(a),(b),(c) (d),(e),(f)	Prediction of Response for Forced Vibration Tests, Radial Excitation on Roof of Structure
		B_2	(a),(b),(c) (d),(e),(f) and (g)	Dyn. Soil Properties as in Subset B_1, but Change of Soil Properties in Backfill
		B_3	"	Dyn. Soil Properties as in Subset B_2 with "No Embedment"
		B_4	"	Dyn. Soil Properties as in Subset B_2 with "Realistic Embedment"
C	3	C_{h1}	(a),(b),(c) (d),(e),(f) and (g),(h),(i)	Prediction of Response for Horiz. Earthquake Excitation with "Realistic Embedment"
C_{v1}		C_{v1}	"	Prediction of Response for Vert. Earthquake Excitation with "Realistic Embedment
		C_{h2}	(a),(b),(c) (d),(e),(f) (g),(h),(i) and (j)	Dyn. Soil Properties as in Subset C_{h1} but Reduction of Shear Wave Velocity Profile by 10 %

*See List of References

The material damping of reinforced concrete at the low strains expected during the forced vibration tests was estimated to be 0,8 percent (Ref. 25). This value was used in the predictive response computations for the forced vibration experiment. For the earthquake of May 20, 1986, a material damping value of 3,0 percent was used due to the larger strains expected during the earthquake. This value is somewhat lower than that proposed for concrete under OBE loading conditions in the USNRC Reg. Guide 1.61 (Ref. 26).

Soil Model used in Model Set B

The soil model established for model set B was documented in detail in Ref. 6. Hence, only the major features are summarized here. The data used was supplied in Data Packages (a), (b), (e) and (f) (Ref. 15, 16, 19 and 20).

Basic Model Requirements. To investigate soil-structure interaction effects with the computer program BHLUSH/BHBOUND, the soil model has to satisfy certain requirements.

Firstly, the "ground surface" of the soil model needs to be level. Information on surface features in the area of the containment model indicated that a level ground surface may be assumed.

Secondly, the "soil deposit" needs to be horizontally layered. Hence, each layer has to be constant in thickness and extend to infinity in a horizontal direction. The seismic refraction survey (Ref. 16) and the boring information from the subsurface investigations showed that the site is layered fairly horizontally so that the assumption of horizontal layers is justified.

Thirdly, the method of analysis requires a finite "depth" of the soil model. For very deep soil profiles, it is therefore necessary to specify a rigid base deep enough in the soil profile, so that its influence on the response of the structure can be neglected. Because the rock level at the site appears to be at a depth of about 400 m below the ground surface, the soil profile was chosen 62 m deep. It could be shown, that a soil profile with this depth subdivided into 22 layers as shown in Figure 1 was adequate for the forced vibration analysis and that the rigid base had no influence on the response of the structure.

Typical Soil Profile. From the data of the subsurface investigations, a typical profile was established at the site, which consists of three soil layers:

- The top layer - a recent alluvial deposit - is about 15 m thick at the site and consists largely of grey silty fine sands (SM) occasionally interbedded with grey fine sandy silts and clays of low plasticity (ML). Typical N-values are in the order of 5 to 15.
- The second layer - also a recent alluvial deposit - is about 20 m thick at the site and consists largely of grey fine to medium sands and some gravels (SP, GP). Typical N-values are in the order 25 to 50.
- The third layer - of Pleistocene age - consists largely of grey silts turning to grey silty clays (ML, CL). It reaches a depth of about 400 m under the containment model, where it is underlain by the Miocene basement rock. Typical N-values up to a depth of 60 m are in the order of 20 to 30.

Physical Soil Properties. The soil properties selected for each of the 22 soil layers, i.e. total unit weight, maximum shear modulus to represent elastic soil stiffness at very low strains, minimum damping ratio to represent material damping at very low strains and Poisson's ratio are given in Table 2.

The choice of the total unit weight values was based on results obtained in laboratory tests and on the classification of soils reported in the boring logs. Table 2 shows that a weight of 19'000 N/m^3 was selected for the more silty and clayey layers and 19'500 N/m^3 for the more sandy and gravelly deposit. Maximum shear moduli were computed from the total unit weight and from the shear wave velocity profile shown in Figure 2, which represents the average of five cross-hole surveys conducted at the site of the 1/4-scale containment model. The average shear wave velocity begins at about 100 m/s at the surface and reaches a value of about 300 m/s at 60 m depth. In the proposed soil model for model set B however, the computed variation with depth of the maximum shear moduli was smoothed out and represented by the following two straight lines:

for $0\ m \leq z \leq 30\ m$

$$G_{max}(z) = 3 + 11 \cdot (z/30)\ (10^4\ kN/m^2)$$

for $30\ m \leq z \leq 60\ m$

$$G_{max}(z) = 14 + 4 \cdot \left(\frac{z-30}{30}\right)\ (10^4\ kN/m^2)$$

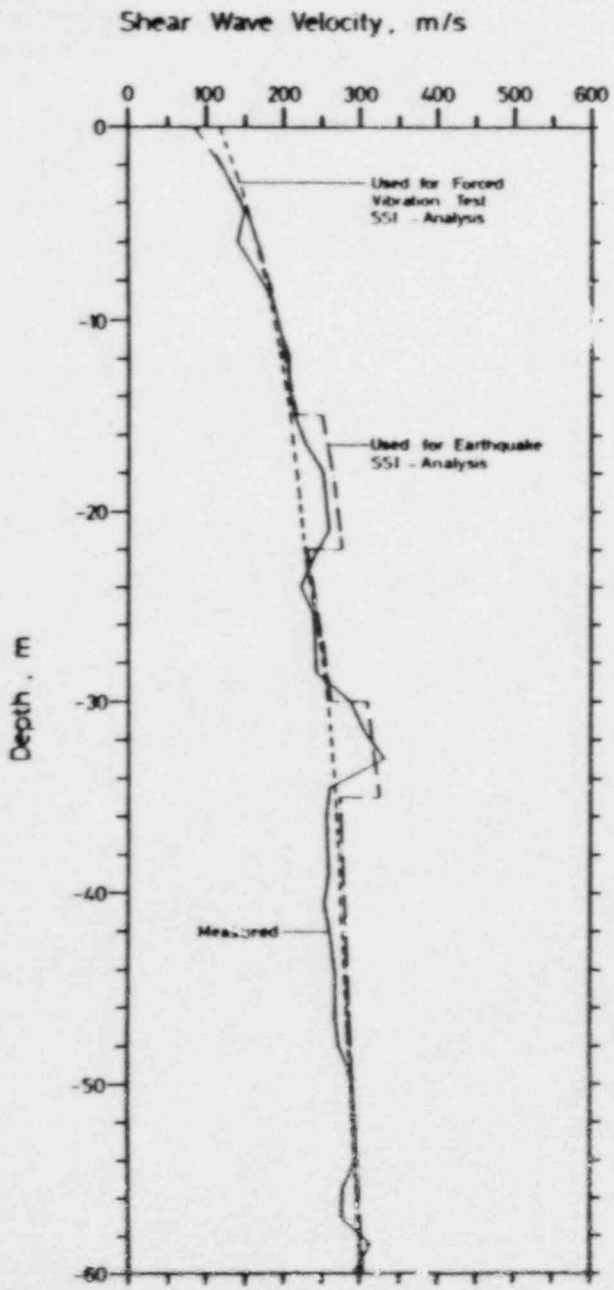

Figure 2. Average Shear Wave Velocity Profiles for Site and Model Sets B and C

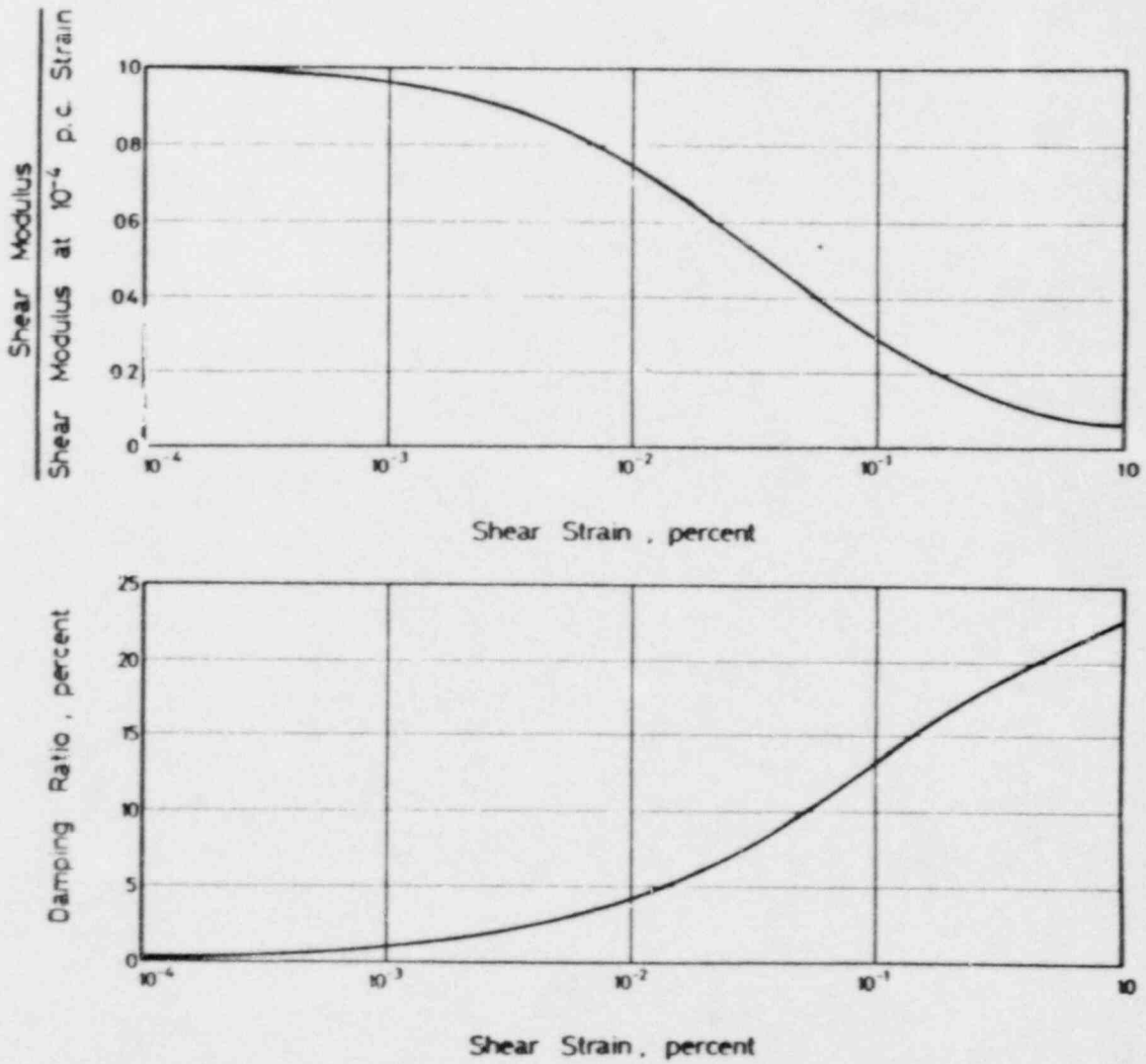

Figure 3. Strain Dependence of Dynamic Soil Properties

Table 3

SOIL PROPERTIES USED IN FRRE-FIELD OF MODEL SET C

Layer No.	Layer Thickn. (m)	Unit Weight (N/m^3)	Shear Modulus at Low Strain (kN/m^2)	Strain Compat. Shear Modulus (kN/m^2)	Damping Ratio (%)	Poisson's Ratio Horiz.	Vert.
1	0,66	18'500	14'195	12'130	2,9	0,480	0,483
2	1,00	18'500	19'549	12'960	5,6	0,483	0,489
3	1,00	18'500	26'018	14'737	7,1	0,486	0,492
4	1,00	18'500	32'447	16'841	8,0	0,488	0,494
5	1,06	18'500	39'067	19'085	8,7	0,489	0,495
6	1,28	18'500	46'519	21'712	9,2	0,491	0,496
7	1,70	18'500	55'100	23'361	9,9	0,492	0,497
8	1,80	18'500	61'500	23'995	10,8	0,493	0,497
9	1,80	18'500	68'100	24'767	11,4	0,492	0,497
10	1,80	18'500	74'700	25'992	11,8	0,491	0,497
11	1,90	18'500	81'200	27'201	12,1	0,491	0,497
12	2,30	20'000	133'400	62'222	8,9	0,486	0,493
13	2,30	20'000	141'900	64'161	9,2	0,485	0,493
14	2,40	20'000	150'500	66'349	9,5	0,484	0,493
15	1,60	20'000	113'600	57'653	12,4	0,488	0,496
16	1,60	20'000	119'500	59'561	12,2	0,488	0,496
17	1,60	20'000	125'300	42'217	12,0	0,487	0,496
18	1,60	20'000	131'200	44'536	12,0	0,485	0,495
19	1,60	20'000	137'100	46'608	12,0	0,485	0,495
20	2,50	20'000	202'400	93'365	9,0	0,478	0,490
21	2,50	20'000	211'700	96'800	9,1	0,477	0,490
22	6,00	19'000	151'200	59'330	10,0	-	0,493
23	6,00	19'000	158'850	63'158	10,0	-	0,493
24	6,00	19'000	166'500	67'000	10,0	-	0,492
25	7,00	19'000	174'640	71'150	10,0	-	0,492

tests reported in Data Packages (e) and (h) (Ref. 19, 22) as well as from other published data (Ref. 11).

Finally, the backfilled excavation pit was not taken into account in model set C.

COMPARISON OF PREDICTIONS WITH MEASUREMENTS FOR VIBRATION TESTS

Predictive Computations

The model subset B1 shown in Figure 1 was used to predict the response of the structure to forced vibrations. The response was calculated for an excitation on the roof in the radial direction only because the computer code BHLUSH/BHBOUND can not handle tangental excitations. The driving point was nodal point 13 (see Figure 1). Contrary to the frequency dependent force amplitude during the tests, the predictive computations were made for a constant force amplitude of 98 kN over the frequency range between 0 and 30 Hz. This is consistent with the results of the vibration tests scaled to a force of 98 kN (Ref. 18, 21). No iteration was performed to obtain strain-compatible soil properties.

The response of the structure was obtained in form of displacement transfer functions at nodal points 16, 1, 67, 117 and 25 (see Figure 1) for the specified output directions normalized to a force of 98 kN. The nodal points with their associated output directions and the corresponding recording channels are given in Table 4.

The displacement transfer functions (displacement and phase) predicted for channels 2 and 3 at the top edge of the structure and for channels 12 and 13 on the basemat are shown in Figures 4 through 7. Channels 2 and 12 recorded in the radial direction, channels 3 and 13 in the vertical direction. The frequency range shown in Figures 4 through 7 was from 0 to 18 Hz only, because the measurements did not show any significant response of the structure above 18 Hz. The maximum displacements predicted at all relevant recording channels are given in Table 4.

The analysis method used to predict the displacement transfer functions did not give modal parameters directly. From the transfer functions however, the most significant mode of vibration can be identified by the marked resonant peak as a rigid body rocking mode. For this mode, the resonant frequency and the modal damping ratio have been determined as 4,64 Hz and 23 %, respectively. The corresponding mode shape is displayed in Figure 8.

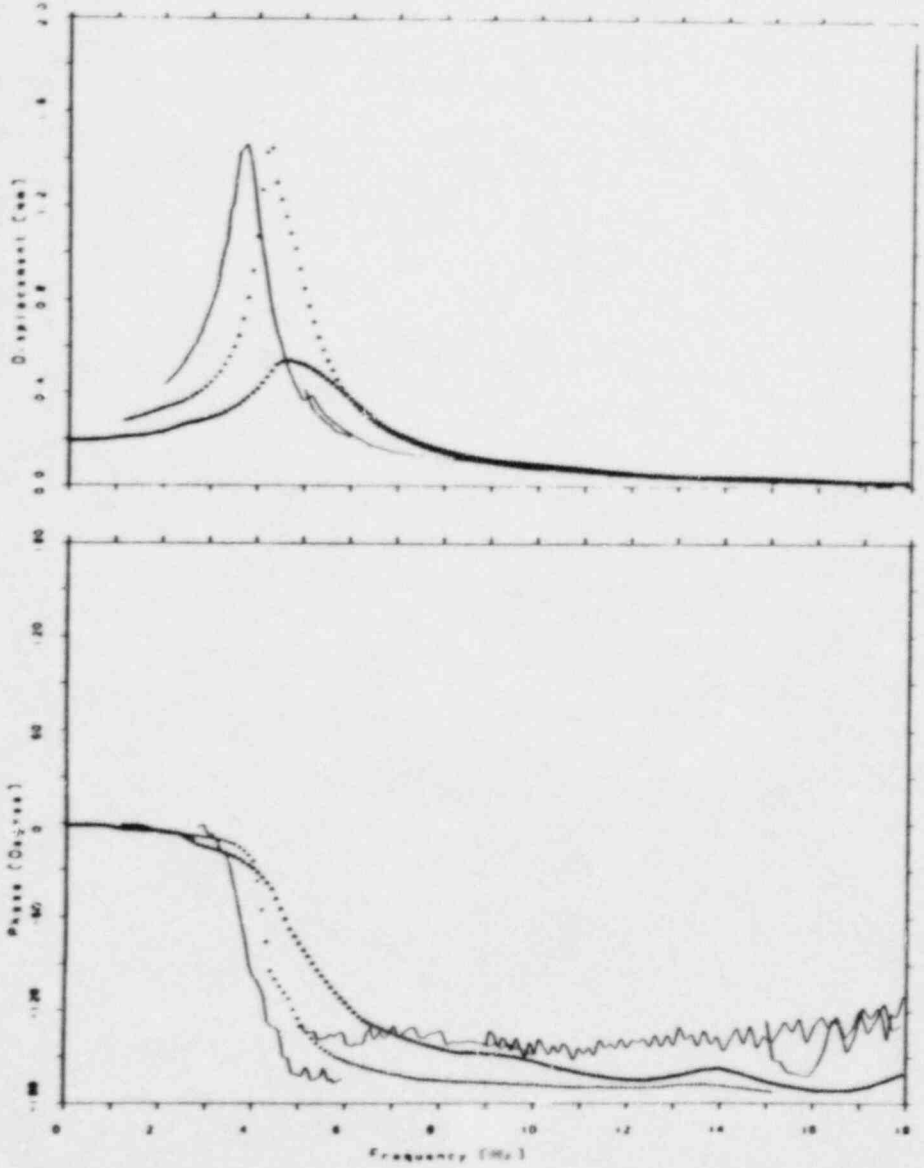

Figure 4. Normalized Displacements and Phases at Channel 2 from Field Measurements (——) and from Models B_1 (▲▲▲) and C_{h1} (+++)

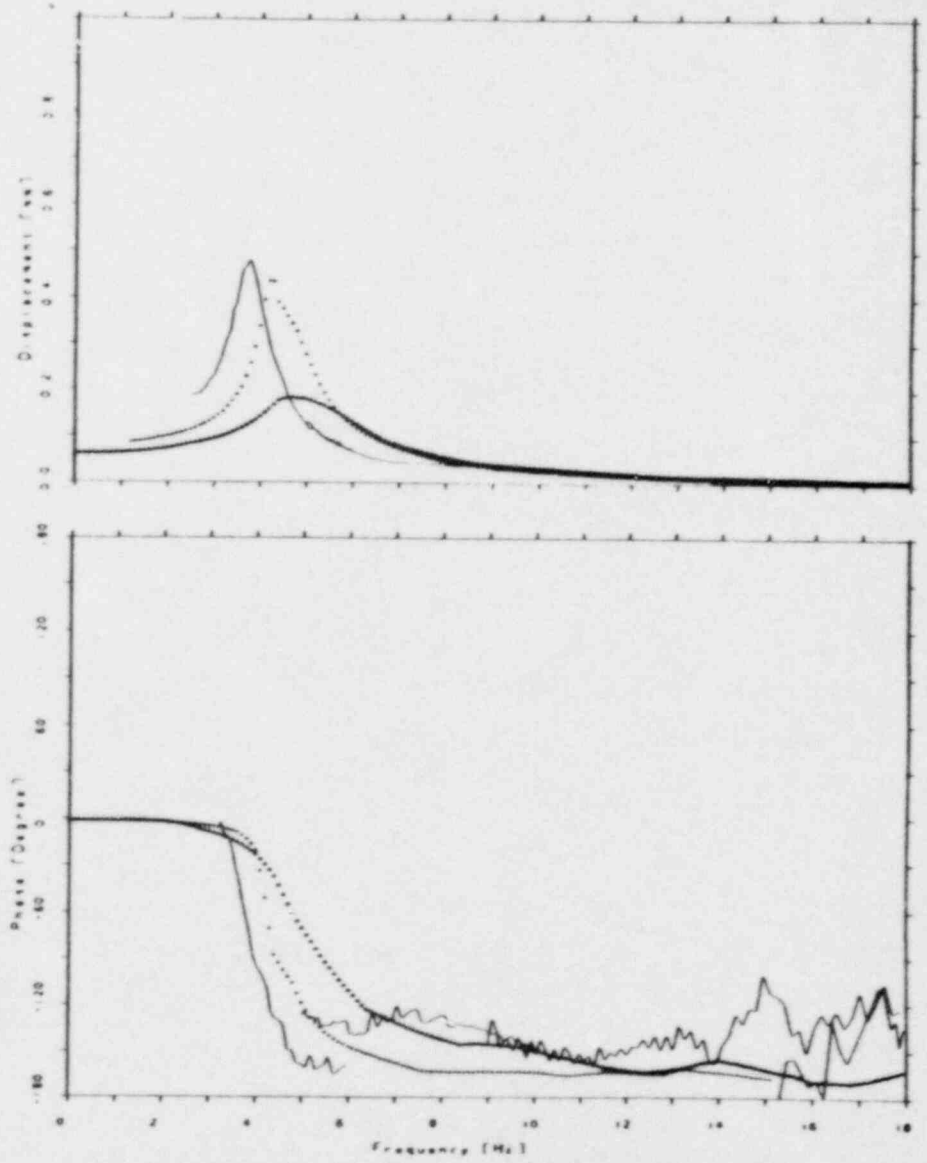

Figure 5. Normalized Displacements and Phases at Channel 3 from Field Measurements (——) and from Models B_1 (▲▲▲) and C_{h1} (+++)

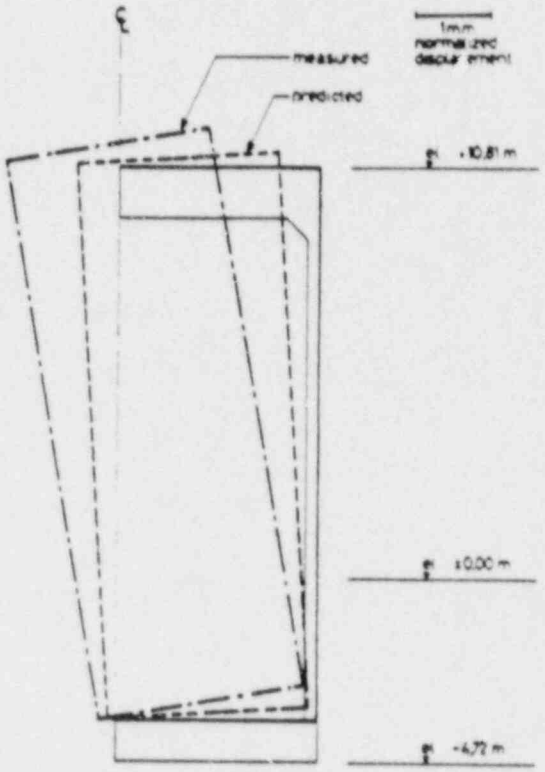

Figure 8. Measured and Predicted Mode Shapes for Rocking Response

The comparison of measured and predicted transfer functions shows that the measured overall behaviour of the soil-structure system could be reproduced in a qualitative way by the predictive computations. The only resonance peak over the frequency range of 0 to 18 Hz - indicating a rigid body rocking of the 1/4-scale containment model - was predicted by the analysis, although there are considerable differences as far as the resonant frequency and the displacement amplitude at resonance are concerned.

From a quantitative comparison of the measured and predicted results, the following differences can be identified:

- The predicted resonant frequency of 4,64 Hz overestimates the measured value of 3,77 Hz (Ref. 21) by about 23 %, indicating a model behaviour which is too stiff.

- The modal damping ratio estimated from the predicted transfer functions is about 23 %. This compares with a measured value of about 10 % (Ref. 21). Taking into consideration, that material damping is not very important at the low strain levels generated during the vibration tests, it is concluded that radiation damping in the model is considerably overestimated.

face. However, soils by nature have a much larger compressive than tensile stiffness. Therefore, the above desribed modelling of the embedded structure seems to tie the structural model much more rigidly into the ground than is the case in reality. Consequently, the computed rocking response is considerably smaller than the measured one (see Figure 8).

To study the effects of embedment, model subset B_2 was changed by making the four soil elements 115, 116, 117 and 118 immediately adjacent to the structure (see Figure 1) very weak with a shear modulus of 100 kN/m^2. Hence, the embedment of the structure was relaxed "completely" (see Table 1, model subset B_3). The computed response of this model showed a resonant frequency of 3,4 Hz which falls below the measured value of 3,77 Hz and a model damping ratio of 5 % which is less than the measured 10 %. The computed displacement amplitude at resonance is now about 3 times larger than the measured value.

The effectiveness of this change showed the importance of a proper modelling of the embedment. Therefore, a final attempt to model the embedment of the structure as realistically as possible was made (see Table 1, model subset B_4). The top soil element 115 adjacent to the structure (see Figure 1) was left weak as in model subset B_3, i.e. 100 kN/m^2. The shear moduli of the underlying three elements 116, 117 and 118 were set equal to 1/4, 1/2 and 3/4 of the values in the free field. The reasoning behind this assumption is, that a rocking structure will most likely develop small gaps between soil and structure near the ground surface, because the soil-structure interface can not carry tension there. Further down in the soil, the overburden pressure is responsible for a soil-structure interface prestressed in compression. Hence, the development of a gap due to the rocking structure will be less likely with increasing depth, until the soil-structure interface behaves as if soil and structure elements were connected to each other. At this point "full" embedment becomes active and the stiffness of the real system is represented by the model. With this model subset B_4 the computed resonant frequency, modal damping ratio and maximum displacement amplitude on the roof at resonance now have values of 4,25 Hz, 8,8 % and 1,63 mm, respectively. These values agree quite well with the measured ones (see Table 4).

Dynamic Soil Properties at Site. As mentioned previously, the dynamic soil properties in the free field for model set C (see Table 3) were slightly changed from their original values in model set B to reflect the additional knowledge from a review of the shear wave velocities used for model set B and from a review of addi-

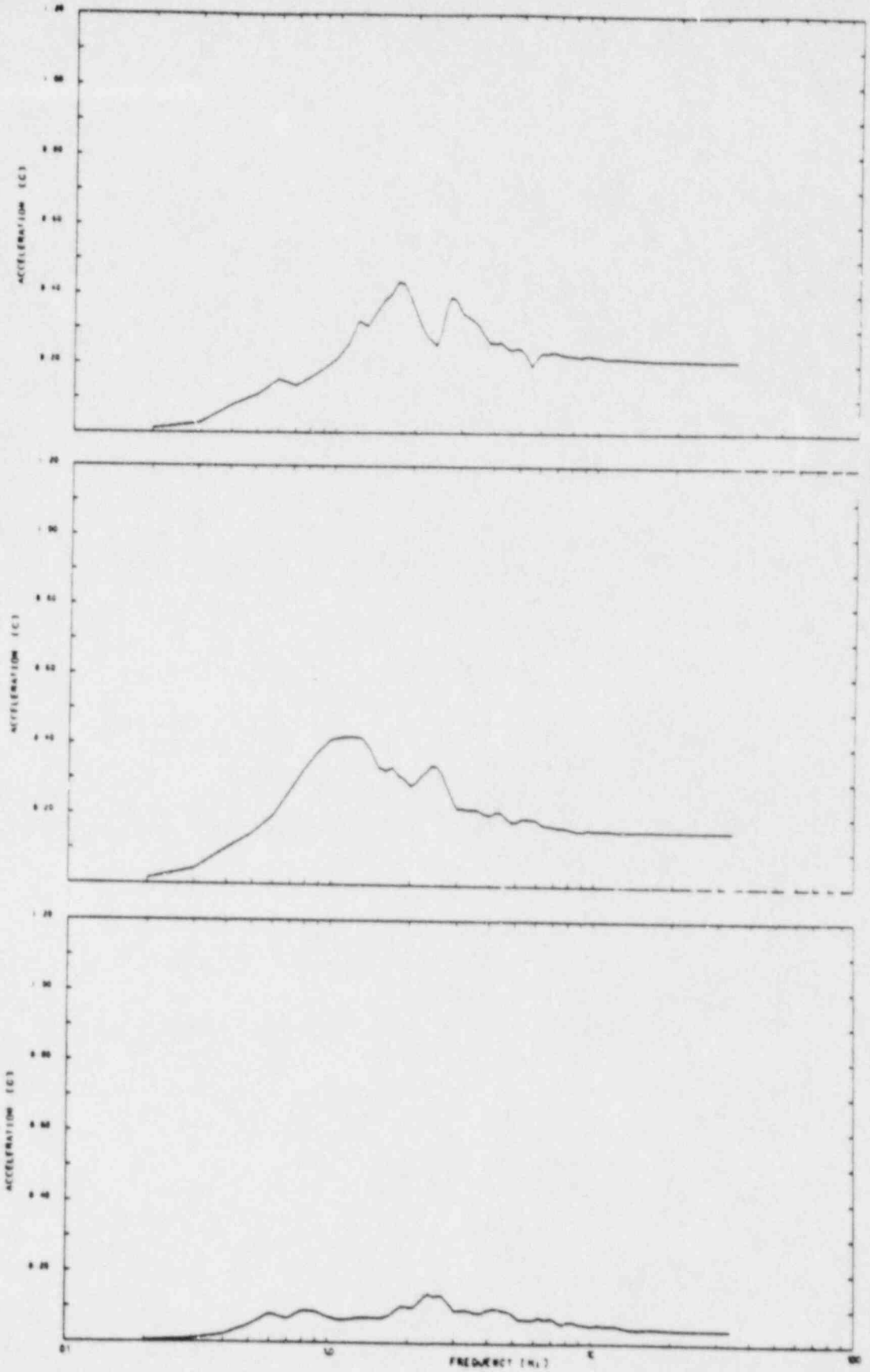

Figure 9. Acceleration Response Spectra of Earthquake Input at Station FA1-5 (Top: N; Middle: E; Bottom: V; Damping: 5 %)

Table 5

MEASURED AND PREDICTED MAXIMUM ACCELERATIONS

Station Code	Nodal Pt.No. C_n	Nodal Pt.No. C_v	Maximum Accelerations in Direction North A_m (cm/sec^2)	North A_p (cm/sec^2)	East A_m (cm/sec^2)	East A_p (cm/sec^2)	Vertical A_m (cm/sec^2)	Vertical A_p (cm/sec^2)
F4UN	21	21	210	200,2	200	181,3	- 64	45,1
F4UE	21	21	212	200,0	204	181,4	41	40,7
F4US	21	21	211	200,2	200	181,3	69	- 52,8
F4UW	21	21	209	200,0	202	181,4	84	47,0
F4LN	113	129	?	170,4	?	154,4	?	- 43,9
F4LE	113	129	127	170,5	147	154,4	40	39,8
F4LS	113	129	126	170,4	148	154,4	69	- 50,7
F4LW	113	129	124	170,5	148	154,4	82	46,7
FA1-1	130	150	130	188,2	157	161,4	47	37,6
FA2-1	130	150	163	207,4	158	156,9	- 44	38,9
FA3-1	130	150	134	203,9	162	161,2	58	44,6
FA1-2	174	202	172	197,9	157	159,2	40	38,3
FA2-2	174	202	207	214,9	160	157,2	69	39,3
FA3-2	174	202	155	205,5	146	161,0	51	42,4
FA1-3	237	277	224	213,3	159	154,8	44	39,7
FA2-3	237	277	211	217,0	166	155,9	46	40
FA3-3	237	277	185	209,9	?	157,7	47	40,8
FA1-4	279	327	200	212,5	156	154,9	43	40,5
FA2-4	279	327	-	214,1	-	155,9	-	40,6
FA3-4	279	327	203	216,0	164	154,8	44	39,6
DHA6	180	208	110	156,3	151	148,3	43	37,7
DHA11	183	211	93	128,1	130	128,0	36	38,4
DHA17	186	214	78	110,1	110	101,4	34	39,1
DHA47	-	-	86	-	83	-	33	-
	Free Field Layer No:							
FA1-5	1		203	203,6	154	154,3	40	39,4
FA2-5	1		189	203,6	155	154,3	42	39,4
FA3-5	1		194	203,6	182	154,3	41	39,4
DHB6	7		135	154,2	150	145,9	39	39,3
DHB11	10		107	125,1	114	129,2	39	39,2
DHB17	13		90	109,5	100	102,3	36	39,2
DHB47	24		97	-	79	-	31	37,9

Note: Am: Measured Acceleration Values

Ap: Predicted Acceleration Values

were computed for the entire profile from the strain-compatible shear wave velocities to agree with the compression wave velocities described before. The variation with depth of the maximum vertical accelerations is also plotted in Figure 10 to a depth of 60 m.

Measured and predicted maximum accelerations in the free-field for all three directions (N, E and V) are given in Table 5. Measured and predicted acceleration response spectra at 5 % damping for stations DHB6 (N, E and V) and DHB47 (only V) are shown in Figures 11 and 12, respectively.

It is concluded that the predicted responses in the free-field compare quite well with the field measurements. An exception to this general conclusions may be the response due to the horizontal N-component for which the maximum accelerations at depth are overestimated. The following may account for this: The soil profile used for the free-field analysis was strain-compatible with the E-component. As already mentioned, this profile is softer and has greater damping ratios as the strain-compatible profile for the N-component. At greater depth this possibly leads to an overamplification of the higher frequencies of the N-component and results in too high predicted maximum accelerations.

Finally, it is noted that the analysis method used does not account for horizontal spatial variation of the free-field motion. Thus, the predicted responses in the free-field at the two surface stations FA2-5 and FA3-5 are identical to the earthquake input motion at station FA1-5. The measured motions, however, shows a certain horizontal spatial variation (see Table 5).

SSI-Analysis

The SSI-Analysis of the soil-structure system was conducted separately for each of the three components (E, N and V) of the earthquake excitation specified at station FA1-5 in the free field. The cut-off frequency was 15 Hz as for the free-field analysis.

Firstly, an initial solution of the soil-structure system represented by the model subset C_{h1} (see Figure 1) was obtained for the E-component of the earthquake input motion. The strain-compatible dynamic soil properties as determined in the corresponding free-field analysis were used. From this solution, the strains in the soil accounting also for the interaction effects of the structure in addition to the effects of the free-field motion, were calculated to a depth of 22 m below the

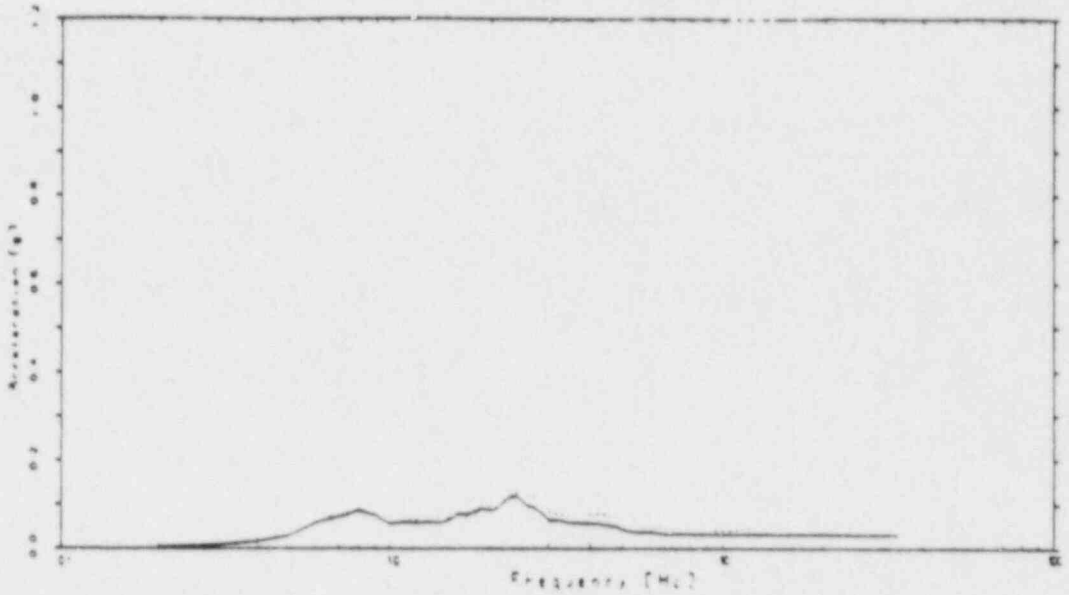

Figure 12. Measured (——) and Predicted (---) Acceleration Response Spectra in Free-Field at Station DHB47 (Vertical Direction; Damping: 5 %)

ground surface. Then, new strain-compatible shear moduli and damping ratios were evaluated for this portion of the soil model. Using these new dynamic soil properties, a second solution was computed, resulting in the final response of the soil-structure system due to the E-component of the earthquake input motion.

Secondally, the same soil properties - including the effects of secondary non-linearities described above - were used to compute the response of the soil-structure system (model subset C_{h1}) due to the N-component of the earthquake input motion.

Thirdly, the vertical solution of the soil-structure system (see Figure 1, model subset C_{v1}) was obtained for the V-component of the earthquake input motion.

Because of the cylindrical coordinates used in the axisymmetric finite element program BHLUSH/BHBOUND, the solutions for each of the three SSI-analyses were obtained in terms of radial, tangental and vertical response components at a point of interest. Hence, to obtain the response in terms of N-, E- and V-components, as they are recorded by the strong motion accelerometers, the radial, tangental and vertical components computed for each of the three SSI-analyses at a specified recording

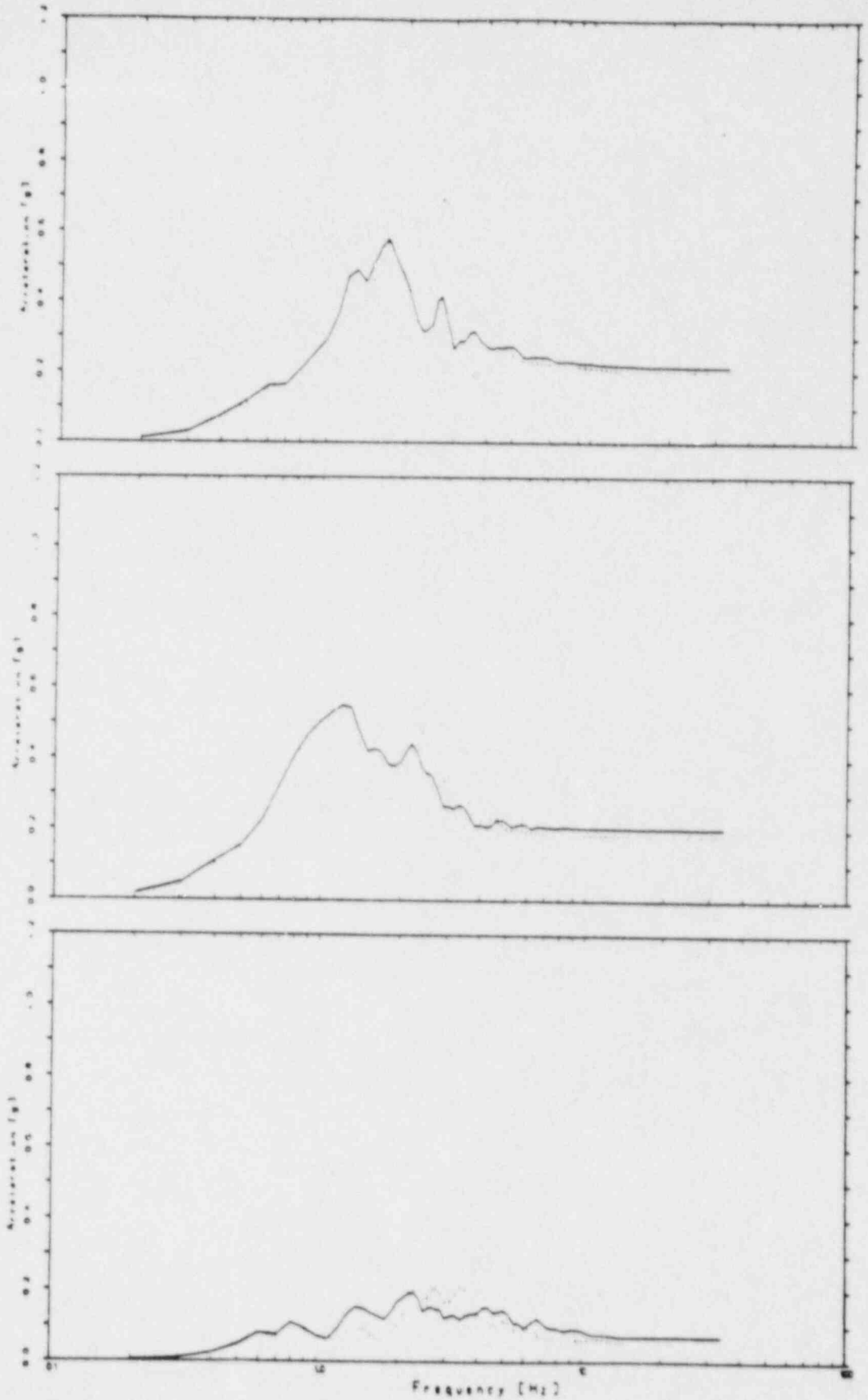

Figure 13. Measured (——) and Predicted (---) Acceleration Response Spectra on Structure at Station F4US (Top: N; Middle: E; Bottom: V; Damping: 5 %)

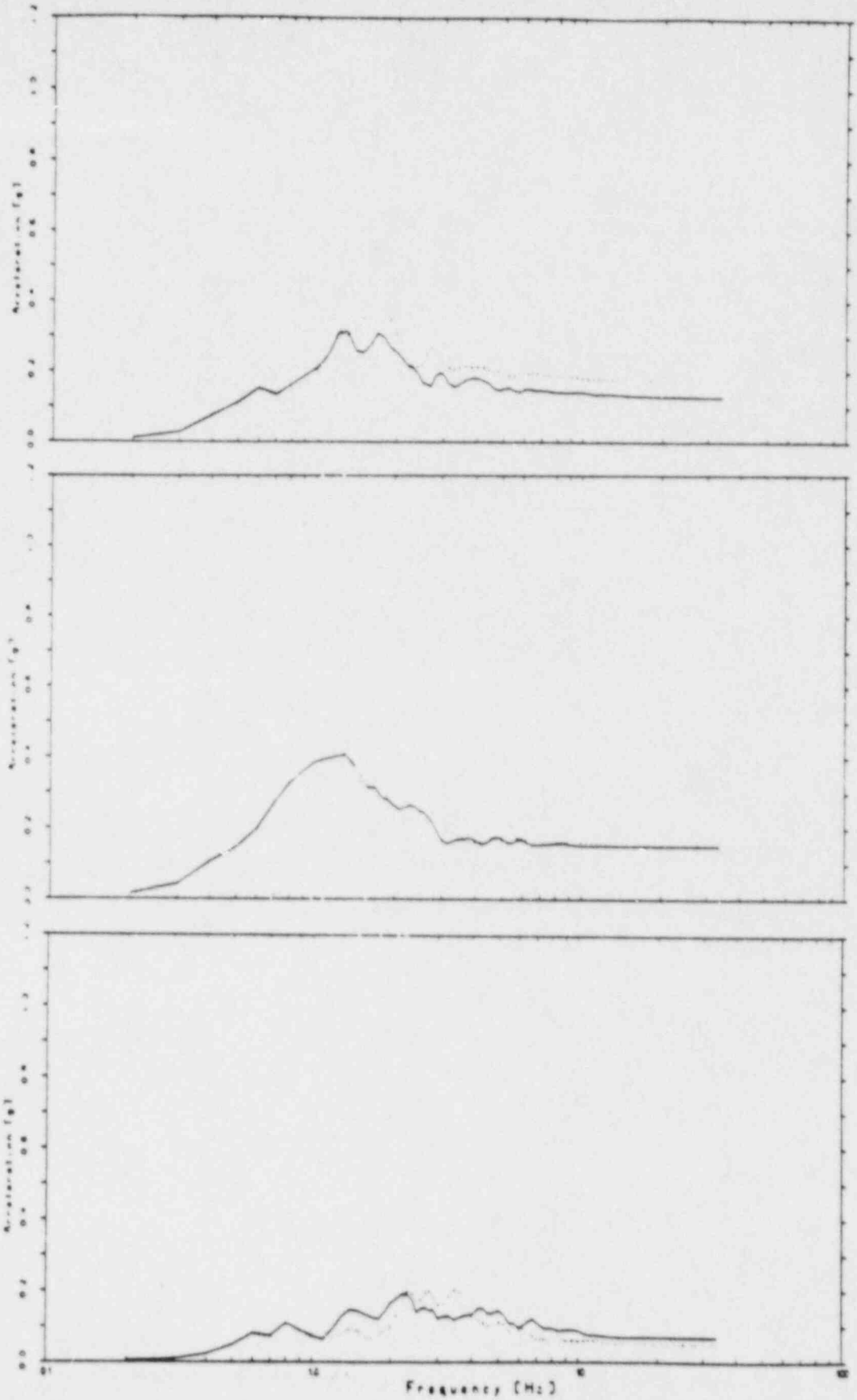

Figure 15. Measured (——) and Predicted (---) Acceleration Response Spectra on Structure at Station F4LS (Top: N; Middle: E; Bottom: V; Damping: 5 %)

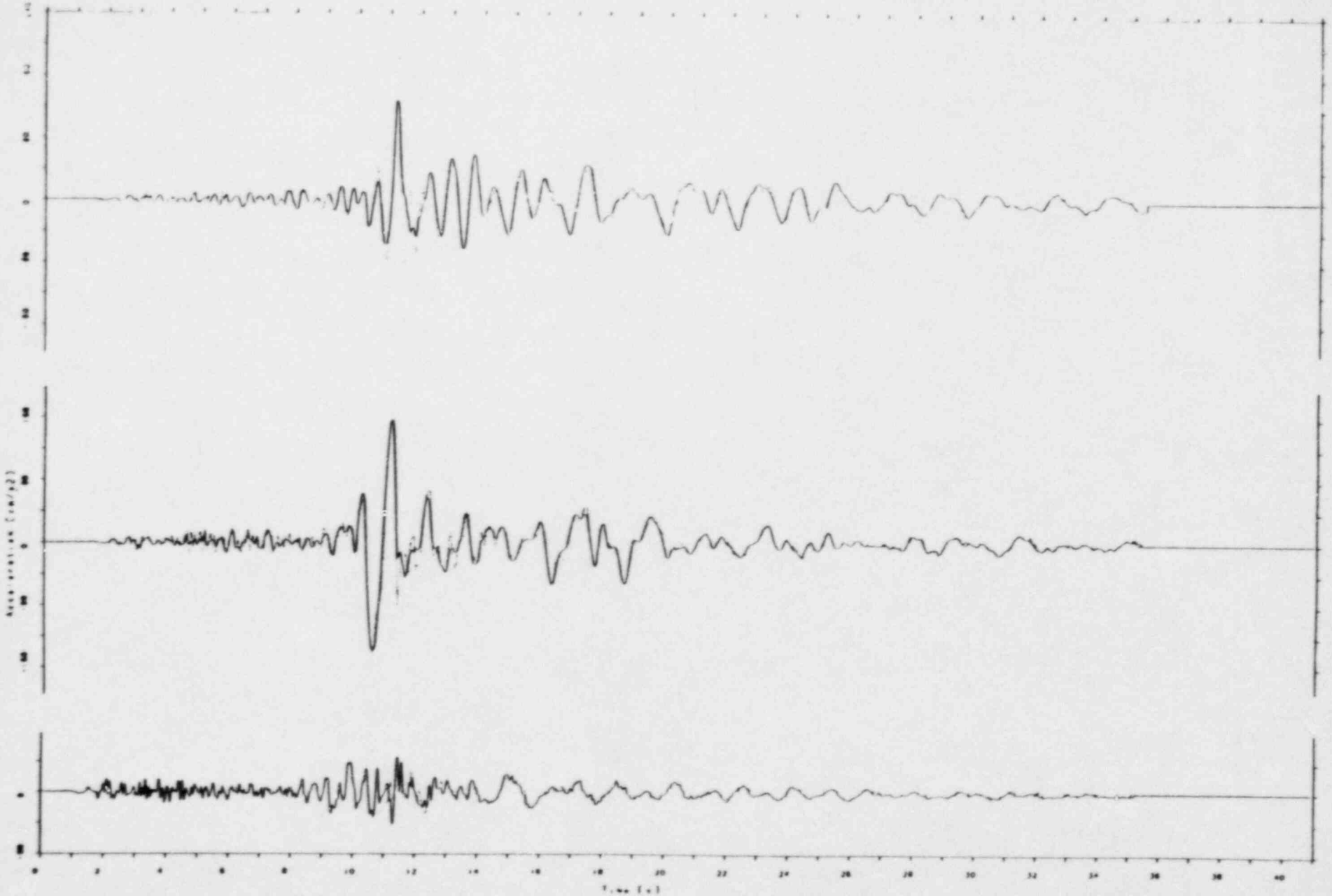

Figure 17. Measured (——) and Predicted (---) Acceleration-Time Histories on Ground-Surface at Station FA1-1 (Top: N; Middle: E; Bottom: V)

A comparison of maximum accelerations in the structure shows (Table 5), that the agreement is better in the E-direction than in the N-direction. While the predicted accelerations at the top of the structure in both horizontal directions deviate between 5 % and 10 % from the measured values, the predicted accelerations at the bottom of the structure in the N-direction are about 35 % larger than the measurements. The E-direction is showing good results. In the vertical direction, the measured accelerations are unterestimated by the analysis both at the top and the bottom of the structure.

In the vicinity of the structure on the ground surface (Stations FA1-1, FA2-1, FA3-1) and immediately underneath the structure (Stations DHA6, DHA11, DHA17), the measured values in the N-direction are again smaller than the predicted ones. The E-direction is showing good agreement. The erratic behaviour of the measured and predicted vertical maximum accelerations in the immediate vicinity of the structure is difficult to interpret.

Approaching the free field, the results at the ground surface improve, which is self-evident with the earthquake input motion specified in the free field. The variation of the maximum accelerations with depth was predicted more accurately in the E-direction and the vertical direction than in the N-direction.

The acceleration response spectra (Figures 13, 15 and 16) show the most obvious differences between measured and predicted responses in the N-direction at the top of the structure (see Figure 13). The marked peak at about 2,8 Hz most likely results from the predicted rocking frequency of the structure. The larger response computed at this frequency can also be observed on other horizontal and vertical acceleration response spectra (see Figures 15 and 16). To show the existence of this rocking frequency in model subset C_{h1} in a more transparent way, the predicted amplitude transfer function between the N-components of Station FA1-5 in the free-field and Station F4US at the top of the structure is plotted in Figure 20. It shows quite well the resonant frequency at 2,8 Hz.

The acceleration-time histories plotted in Figure 14 also shows that the computed oscillations at about 2,8 Hz following the main peak response are much stronger than in the measured acceleration time history. This indicates that rocking at this frequencys may not be as important in the field as predicted by the computations, or rocking in the field may take place at an other frequency. Furthermore, the N-com-

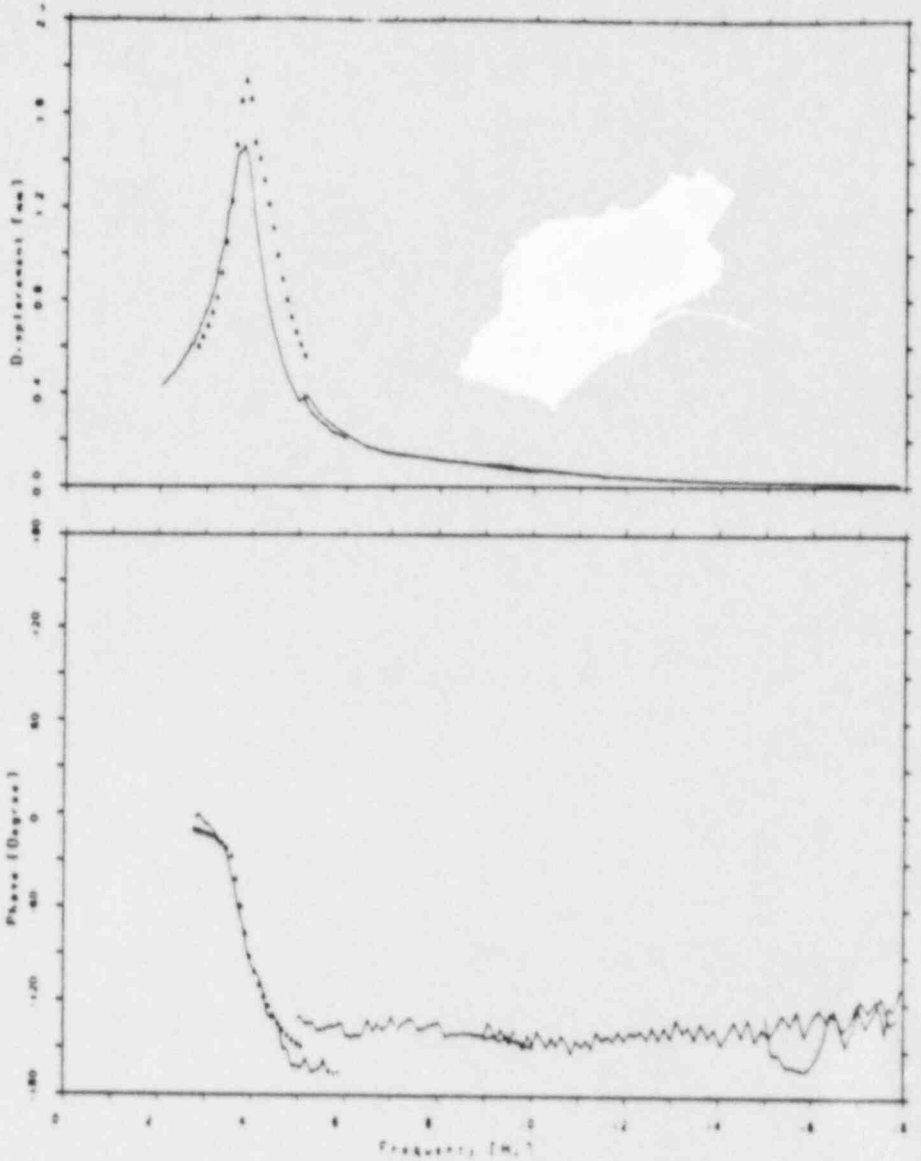

Figure 19. Normalized Displacements and Phases at Channel 2 from Field Measurements (——) and from Model C_{h2} (▲▲▲)

Compared to the measured behaviour, model subset C_{h2} seems still somewhat too stiff. From the measured transfer function the maximum amplification is estimated to be between about 2,0 and 2,2 Hz. The softer soil profile led however to a partial improvement of the predicted results as shown by the accelaration response spectra and acceleration time histories displayed in Figures 21 and 22.

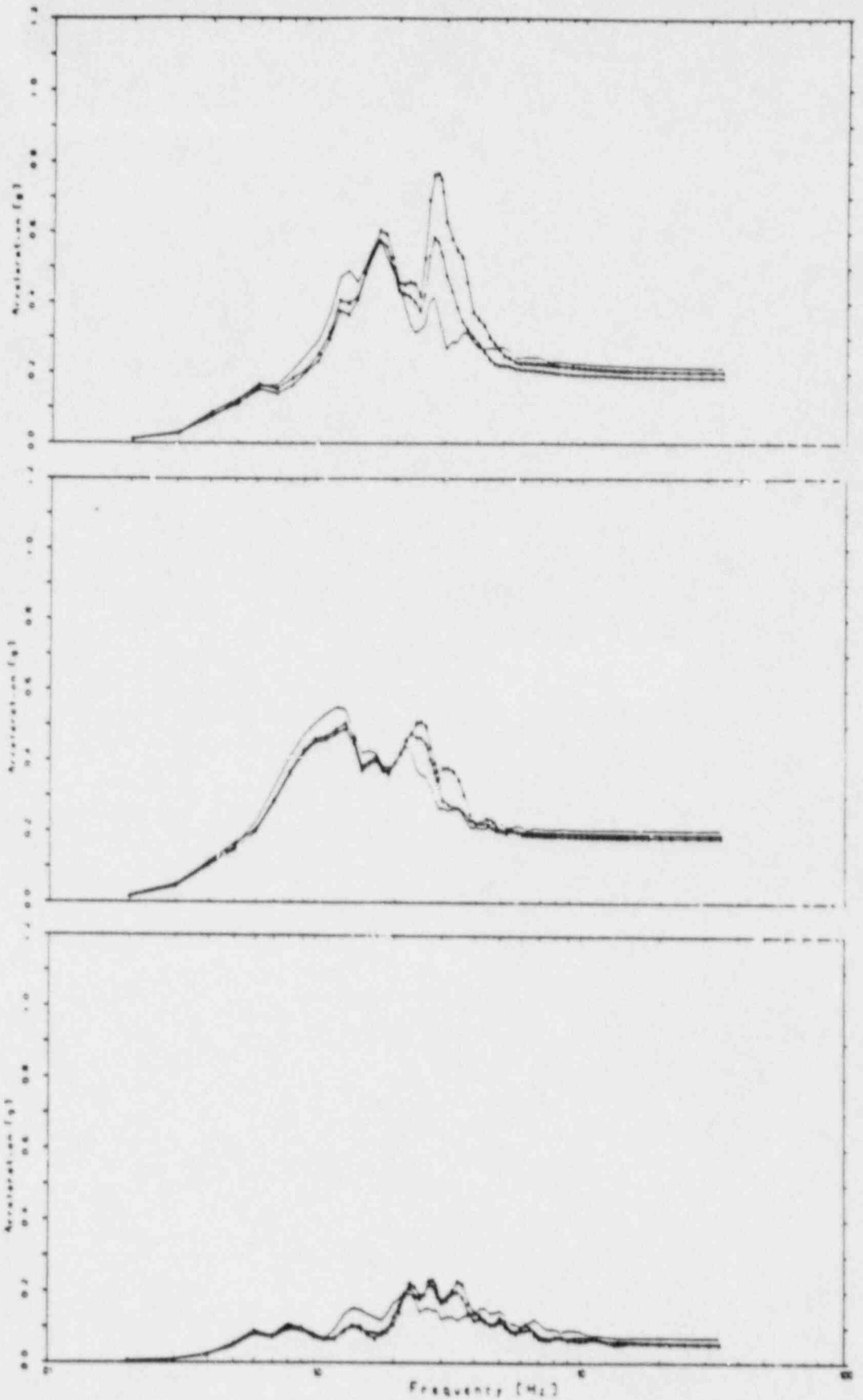

Figure 21. Acceleration Response Spectra on Structure at Station F4US from Field Measurements (——) and from Models C_{h1}(▲▲▲) and C_{h2}(+++) (Top: N; Middle: E; Bottom: V; Damping 5 %)

gained through the project will certainly be helpful in the analysis of futur SSE-problems.

It is our oppinion, that the differences observed between measured and predicted responses can be attributed mainly to uncertainties about the parameters used in the analysis. These uncertainties result mainly from the inability to determine correctly the dynamic soil properties and to translate measured or estimated system properties into appropriate model parameters. To minimize the effects of these uncertainties on the predicted response, a good portion of experience is required.

The question about the usefulness of forced vibration tests to improve earthquake response predictions has been answered positively, based on the experience gained during this project. The results of the forced vibration tests were very helpful in refining model subsets B_1 through B_4. Furthermore, as good a match as possible between measured and predicted results for forced vibration tests tends to improve the predicted earthquake response.

Finally, some findings worth mentioning were made during the course of this project:

- The SSI-methodology used during this project reaches its limits for very soft and deep soil profiles. To reproduce correctly the behaviour of the soil, the layers in the model should be chosen very thin. This is particularly important in deconvolving correctly the earthquake motion in the free-field. However, this requirement may be in conflict with the computer time required to solve the problem.

- The measured free-field response in the N-direction suggests that the use of independent strain-compatible soil properties for each direction improves the prediction of the response in the free-field and therefore also the response of the soil-structure system. This should be further investigated.

- The comparison of measured and predicted responses in the structure indicates that the soil underneath the structure may be softer than used in the analysis. A rocking frequency of the structure around 2 Hz could in our opinion further improve the prediction of the structural response.

In conclusion, it is hoped that the participation of HSK in the USNRC Validation Project has resulted in some valuable contributions in regard to the validation of SSI-methodologies. Throught this participation, HSK has improved its understanding of SSI-methodologies used in the analysis of nuclear power plants.

15. Data Package (a). First Phase Soil-Boring Test Data.

16. Data Package (b). SMART-1 Array Geological Data.

17. Data Package (c). Structural and Geometric Details of the 1/4-Scale Containment Model and Instrument Locations.

18. Data Package (d). Vibration Test Input Data.

19. Data Package (e). Soil Test Data-Phase 2.

20. Data Package (f). Geological Data from Within Array of Model Structure.

21. Data Package (g). Response Data from Vibration Test of Completed Structure.

22. Data Package (h). Additional Information on Soil Testing.

23. Data Package (i). Free-Field Motion from Strong Motion Event of 5/20/86.

24. Data Package (j). Complete Set of Ground Motion and Structural Response Records from 5/20/86 Event.

25. H. Bachmann. "Zur Schwingungsdämpfung teilweise vorgespannter Leichtbeton- und Betontragwerke." Schweizer Ingenieur und Architekt, Nr. 11, 1986.

26. U.S. NRC. "Damping Values for Seismic Design of Nuclear Power Plants." Regulatory Guide 1.61., October 1973.

27. V. Langer, S. Tinic, E. Berger, P. Zwicky and E.G. Prater. "Full Scale Vibration Test on Nuclear Power Plant Auxiliary Building: Part I." Transactions of the 9th International Conference on Structural Mechanics in Reactor Technology, Volume K1, pp. 261, Lausanne 1987.

28. D. Flade, H. Steinhilber and A. Dietz. "Full Scale Vibration Test on Nuclear Power Plant Auxiliary Building: Part II." Transactions of the 9th International Conference on Structural Mechanics in Reactor Technology, Volume K1, pp. 267, Lausanne 1987.

REFERENCES

1. Argonne National Laboratory. "Validation of Soil-Sturcture Interaction (SSI) Methodolgy: EPRI/USRNC Seismic Experiment." Statement of Work, April 1986.

2. Brookhaven National Laboratory and U.S. Nuclear Regulatory Commission. "Proceedings of the Workshop on Soil-Structure Interaction, Bethesda, Maryland, Juni 16 - 18, 1986." NUREG/CP-0054, December 1986.

3. Basler & Hofmann. "Validierung von Analysemethoden zur Lösung von Boden-Struktur-Interaktionsproblemen bei Kernanlagen im Falle von Erdbeben (Validation of Analysis Methods to Solve Soil-Structure Interaction Problems in Connection with Nuclear Installations Subjected to Earthquakes)." Proposal submitted to Swiss Nuclear Safety Department (HSK), September 1986.

4. E. Berger. "Seismic Response of Axisymmetric Soil Structure Systems." Doctoral Dissertation, University of California, Berkeley, 1975.

5. Basler & Hofmann. "BHLUSH/BHBOUND: Computer Program for the Dynamic Analysis of Axisymmetric Soil-Structure Interaction Problems." User's Manual, Rev. 0, December 1986.

6. Basler & Hofmann. "Predictive Response Computations for Forced Vibration Experiments on 1/4-Scale Containment Model in Lotung Taiwan." Progress Report for Phase 1 of HSK Validation Project for Swiss Nuclear Safety Department (HSK), July 1987.

7. Basler & Hofmann. "Comparison of Measured and Predicted Forced Vibration Responses and Prediction of Earthquake Response for 1/4-Scale Containment Model in Lotung, Taiwan." Progress Report for Phases 2 & 3 of HSK Validation Project for Swiss Nuclear Safety Department (HSK), September 1987.

8. Basler & Hofmann. "Comparison of Predictions with Measurements for Vibration Tests and Earthquake of May 20, 1986 at 1/4-Scale Containment Model in Lotung, Taiwan", Final Report of HSK Validation Project for Swiss Nuclear Safety Department (HSK), October 1987.

9. J. Lysmer et al. "FLUSH: A Computer Program for Approximate 3-D Analysis of Soil-Structure Interaction Problems." Earthquake Engineering Research Center, Report No. EERC 75-30, University of California, Berkeley, November 1975.

10. H.B. Seed and I.M. Idriss. "Soil Moduli and Damping Factors for Dynamic Response Analyses". Earthquake Engineering Research Center, Report No. EERC 70-10, University of California, Berkeley, December 1970.

11. H.B. Seed, R.T. Wong, I.M. Idriss and K. Tokimatsu. "Moduli and Damping Factors for Dynamic Analysis of Cohesionless Soils." Journal of Geotechnical Engineering, ASCE, Vol. 112, No. 11, November 1986.

12. J.M. Roesset and R.V. Whitmann. "Theoretical Background for Amplification Studies." Research Report R69 - 15, Massachusetts Institute of Technology, Cambridge, March 1969.

13. P.B. Schnabel et al. "SHAKE: A Computer Program for Earthquake Response Analysis of Horizontally Layered Sites." Earthquake Engineering Research Center, Report No. EERC 72-12, University of California, Berkeley, December 1972.

14. Basler & Hofmann. "FLUSH.F77: Computer Program for the Dynamic Analysis of Soil-Structure Interaction Problems." User's Manual, Rev. 0, December 1986.